BOLETIN DE LA SOCIEDAD ESPAÑOLA DE
Cerámica y Vidrio
www.elsevier.es/bsecv

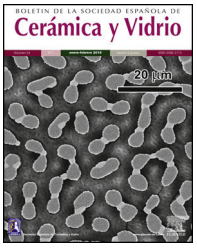

Influence of fly ash and steam on microstructure and mechanical properties of oxide bonded porous SiC ceramics

*Dulal Das, Nijhuma Kayal**

CSIR-Central Glass and Ceramic Research Institute, 196, Raja S.C. Mullick Road, Kolkata 700 032, India

ARTICLE INFO

Article history:
Received 9 October 2018
Accepted 29 May 2019
Available online 22 June 2019

Keywords:
SiC filter
Corrosion
Microstructure
Mechanical strength

ABSTRACT

Ceramic filters specially SiC filters are used in advanced coal combustion and gasification processes to remove fine dust particles from the fuel gas at high temperatures and high pressure for protection of turbine blades and other downstream components from corrosion and erosion and to meet the environmental regulations. Processing of corrosion resistant porous SiC ceramics at low temperature using a simple technique is still challenging. In this study oxide bonded porous SiC ceramics were synthesized by cost effective method. The corrosion behaviour of SiC ceramic filter materials in presence of steam, coal ash and both coal ash and steam was investigated at 1000 °C for 96–240 h. The apparent changes in mass, porosity and density with corrosion duration and environment were recorded. Finally SEM, XRD and mechanical tests of the corroded samples were carried out. The corrosion test results indicated water vapour is the perpetrator for strength degradation.

© 2019 SECV. Published by Elsevier España, S.L.U. This is an open access article under the CC BY-NC-ND license (http://creativecommons.org/licenses/by-nc-nd/4.0/).

Influencia de las cenizas volantes y el vapor de agua en la microestructura y las propiedades mecánicas de las cerámicas porosas de SiC ligadas mediante óxidos

Palabras clave:
Filtro de SiC
Corrosión
Microestructura
Resistencia mecánica

RESUMEN

Los filtros cerámicos, especialmente los filtros de SiC, se utilizan en procesos avanzados de combustión y gasificación de carbón para eliminar las de polvo fino partículas en suspensión del gas combustible, a altas temperaturas y altas presiones, para proteger los álabes de las turbinas, y otros componentes aguas abajo, de la corrosión y la erosión y para cumplir con las regulaciones ambientales. El procesamiento de cerámicas porosas de SiC resistentes a la corrosión a baja temperatura utilizando una técnica simple sigue siendo un desafío. En este estudio, las cerámicas porosas de SiC ligadas mediante óxidos se sintetizaron mediante un método rentable. El comportamiento a la corrosión de los filtros cerámicos de SiC en presencia de vapor de agua, ceniza de carbón y ceniza de carbón y vaporde agua se investigó a 1000° C durante 96-240 horas. Se registraron los cambios aparentes en masa, porosidad

* *Corresponding author.*
E-mail address: nijhuma@cgcri.res.in (N. Kayal).
https://doi.org/10.1016/j.bsecv.2019.05.003
0366-3175/© 2019 SECV. Published by Elsevier España, S.L.U. This is an open access article under the CC BY-NC-ND license (http://creativecommons.org/licenses/by-nc-nd/4.0/).

y densidad con la duración de la corrosión y el medio ambiente. Finalmente se llevaron a cabo estudios de MEB, DRX, XRD y propiedades mecánicas de las muestras corroídas. Los resultados del ensayo de corrosión indicaron que el vapor de agua es el responsable de la degradación de la resistencia mecánica.

© 2019 SECV. Publicado por Elsevier España, S.L.U. Este es un artículo Open Access bajo la licencia CC BY-NC-ND (http://creativecommons.org/licenses/by-nc-nd/4.0/).

Introduction

At present there is considerable interest in advanced clean coal technology such as integrated gasification combined cycle (IGCC) and pressurized fluidized-bed combustion (PFBC) systems for electric power generation because of high energy-efficiency as well as a cleaner environment. Cleaning of flue gas is necessary to prevent the corrosion of the turbine blade by the harmful submicron-sized particles which ultimately increases the energy efficiency in the PFBC system [1]. The PFBC technology operates at a temperature of ~800–900 °C and gas pressure of ~8–10 bar and flue gas generated contains toxic gases like SO_2, CO, NO, NO_2 and fine particulates. Therefore a hot corrosion resistant material is desirable for the hot gas filter. To meet these requirements, SiC ceramic materials have been used as a hot gas filter. In this filter system, cleaning process is essential for the continuous filtration to prevent deposition of dust particles and fouling caused by the agglomeration. It is important to maintain a high cleaning efficiency during long operation of filters in order to reduce pressure drop as well as the operating costs [2]. In this hot gas filtration, high thermal and mechanical durability of porous filters are required to sustain aggressive process environments containing steam, dust, pressure, and gaseous species [3–5]. Characterization of hot gas filtration in coal combustion and gasification systems was intensively described by Alvin et al. [6]. The author also reported a review on the deposits of ash, char and fine sorbent particles on the filters in advanced coal fired processes [7]. The filters were tested in oxidizing pressurized fluidised bed combustion demonstration plants or in integrated combined cycle gasification systems. Microstructure and composition of some SiC based hot gas filter materials were characterized by Pastila et al. [8]. Exposure under simulated combustion environment (high temperature, water vapour and gaseous sodium compounds) [9] caused a decrease in strength, which cause continuous degradation of filter and finally its failure under real operation conditions. However, char, ash or fine sorbent particles can potentially have a toxic impact on the life of porous ceramic filters that are currently used. Therefore, the knowledge of critical points of the porous ceramic filter elements is essential to the successful operation of the hot gas filtration in advanced biomass gasification technology. Clay bonded porous SiC ceramic filters are standard materials for hot gas filtration applications and are well known since many years, but the filter failed due to the depletion of the binder phase in hot gas filtration environments including steam and alkali [9]. In the present study ceramic filter were prepared using alumina additives with reduced amount of clay and investigated the corrosion behaviour of the filter in contact with fly ash and steam to predict suitability of the material as hot gas filter. The corrosion results indicated improvement of corrosion properties with addition of alumina additives.

Materials and methods

Commercial SiC powders (80S, Grindwell Norton Ltd., India; $d_{50} = 212\,\mu m$), alumina powders (Al-HIM, Indian Aluminium Co. Ltd., Howrah, India; α-form; $d_{50} = 6.5\,\mu m$) and graphite powder (Kanodia Minerals & Chemical Co., Howrah, India; $d_{50} = 12.9\,\mu m$) as pore former were used in the present work. Clay mineral (Rajmahal Quartz Sand and Kaolin Co., Kolkata, India, Chemical analysis (in % w/w): SiO_2, 53.6; Al_2O_3, 31.3; TiO_2, 0.7; Fe_2O_3, 0.8; CaO, 0.1; Na_2O, 0.6 and K_2O, 0.2 and LOI, 12.7), Na salt of carboxy methyl cellulose Loba Chemie Pvt. Ltd., Mumbai, India) and calcium carbonate (Merck Specialities Pvt. Ltd., Mumbai, India) was used as sintering aids in 3:2:1 ratio weight ratio. The powder mixture was kneaded well to develop suitable workability for compaction and was pressed at 23 MPa pressure in a stainless steel die to produce rectangular bars ($50 \times 20 \times 16\,mm^3$). The dried samples were heat treated at 1100 °C for burning of graphite pore former and subsequently at 1400 °C for 4 h to produce the oxide bonded porous SiC samples. The sample prepared without and with alumina was named as S and SA respectively. The weight and dimensions of the porous SiC samples were measured; their density and porosity were determined by water immersion technique. Fly ash (CESC Budge Budge, Kolkata) with softening temperature 1380 °C, bulk density 0.8 g/cc, true density 2.4 g/cc was used for corrosion study. The d_{10}, d_{50} and d_{90} of the fly ash were 4.9, 31.2 and 131 μm, respectively. Main chemical constituents present in the fly ash were 59.6% SiO_2, 27.3%

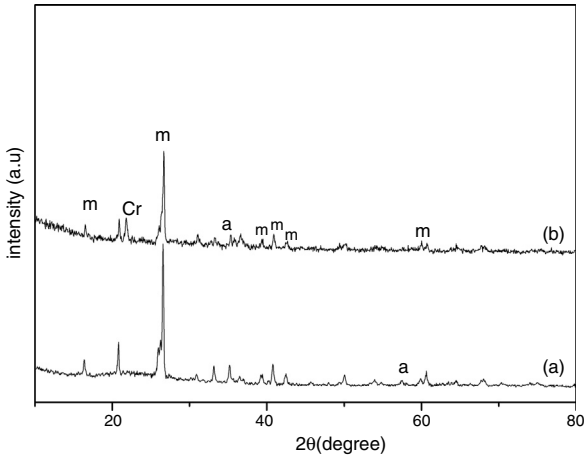

Fig. 1 – XRD analysis of fly ash (a) as received (b) calcined at 1000 °C for 96 h.

Table 1 – Change of mass and porosity of the filter material after corrosion with steam, fly ash in presence or absence of steam.

Sample code	Initial porosity (vol%)	Corrosion for 96 h in presence of						Corrosion for 240 h in presence of			
		Fly ash		Fly ash and steam		Steam		Fly ash and steam		Steam	
		Porosity (vol%)	Mass gain (wt%)	Porosity (vol%)	Mass gain (wt%)	Porosity (vol%)	Mass gain (wt%)	Porosity (vol%)	Mass gain (wt%)	Porosity (vol%)	Mass gain (wt%)
S	37.7	35.4	0.2	32.6	0.8	29.78	1.4	31.2	1.9	30	2.4
SA	33.0	30.6	0.3	28.9	0.65	27.2	0.9	30.6	1.1	28.3	1.7

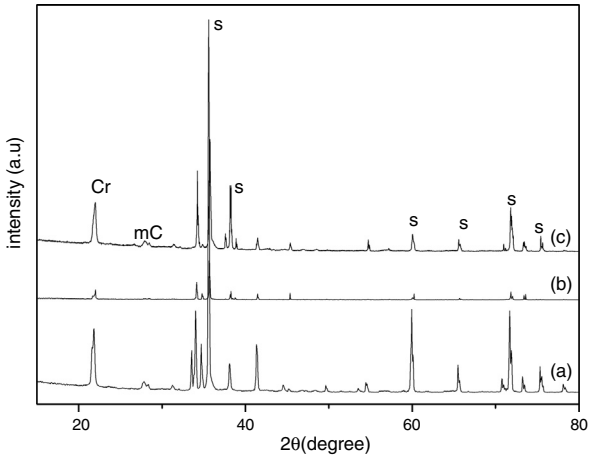

Fig. 2 – XRD plot of S after corrosion with (a) steam, (b) ash, (c) steam and ash (Cr, cristobalite; m, mullite; s-SiC, C-alkaline aluminosilicate).

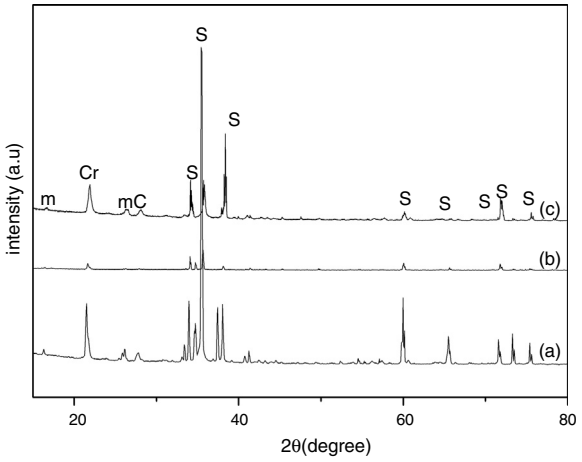

Fig. 3 – XRD plot of SA after corrosion for 96 h with (a) steam, (b) ash, (c) ash and steam.

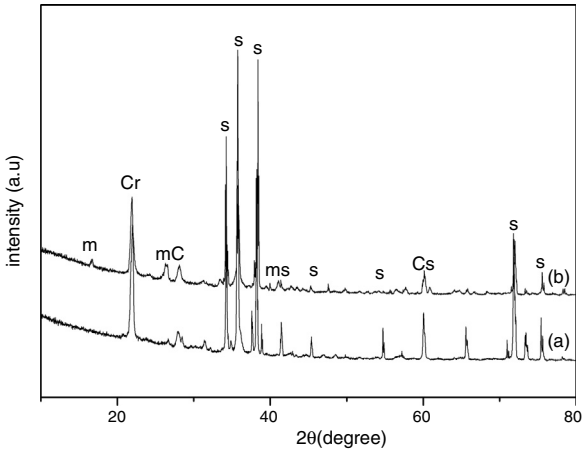

Fig. 4 – XRD pattern of samples after corrosion for 240 h with steam and ash (a) S; (b) SA.

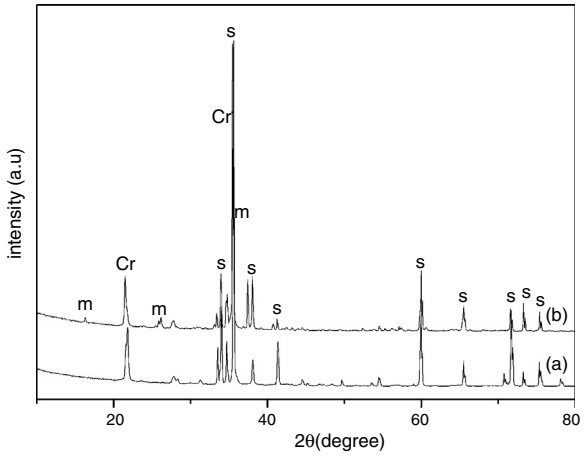

Fig. 5 – XRD pattern of samples after corrosion for 240 h with steam (a) S; (b) SA.

Al_2O_3, 6.3% Fe_2O_3, 1.69 TiO_2, 1% CaO and rest other constituents.

For the corrosion experiments, the samples of each composition covered with fly ash were placed in aluminium oxide boats and was heat treated at 1000 °C for 24–96 h. In another set of experiment corrosion studies were carried out in presence of steam for 96–240 h. For generation of steam, when the furnace temperature was reached to 700 °C, water was injected inside the furnace at a rate of 15 ml/min through water dosing pump. Then furnace temperature was allowed to increase up to 1000 °C and was kept for 96–240 h. The changes in mass, porosity and density of the corroded samples were recorded. Pore size of the samples were determined following Hg intrusion porosimetry; crystalline phase analysis was done by XRD technique and the quantitative analysis was done by the Rietveld technique using the High Score Plus software (version 3.0e, PAN analytical B.V.). The microstructure of the porous SiC samples was examined by scanning electron microscopy (Model SE-440; Leo-Cambridge, Cambridge, UK). Room temperature flexural strength of the samples was determined in a three-point mode (sample size: $4.5 \times 4.7 \times 3.5\ mm^3$; span:

Table 2 – Quantitative estimation of the crystalline phases after corrosion with steam in presence or absence of fly ash for 96 h.

Sample no.	Initial composition of filter material				After corrosion in presence of steam									
					With ash					Without ash				
	SiC	Cr	Mullite	GOF	SiC	Cr	Mullite	Ca–Al	GOF	SiC	Cr	Mullite	Ca-Al	GOF
S	80.4	19.6	–	1.81	69.9	17.2	–	12.9	1.84	74.8	25.2	–	–	1.42
SA	73.7	10.5	15.8	1.68	55.3	22.0	11.1	11.6	2.22	64.7	22.3	13	–	1.98

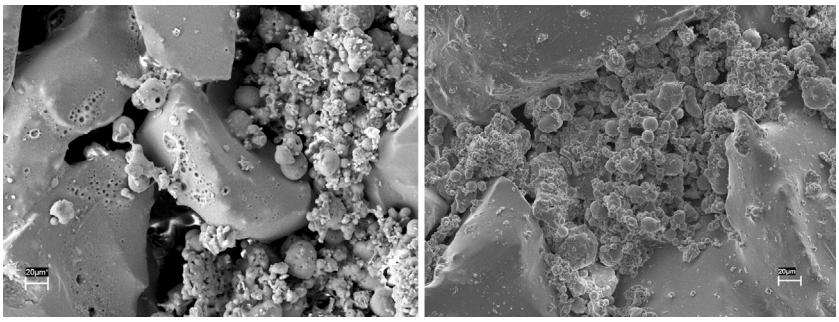

Fig. 6 – FESEM photographs of top surface of sample after exposure at 1000 °C for 96 h covered with fly ash (L) S; (R) SA.

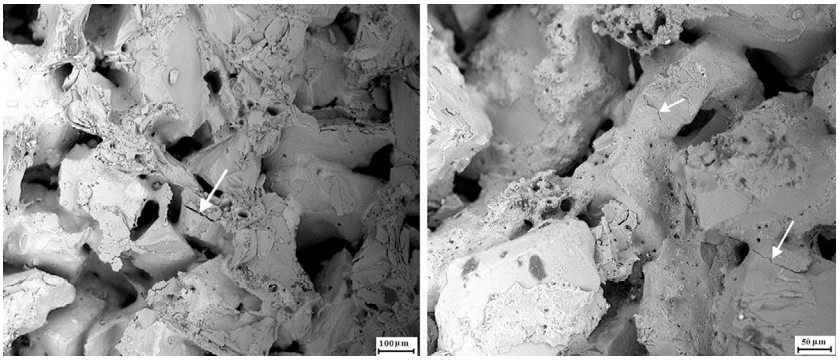

Fig. 7 – SEM photographs of top surface of sample after corrosion with steam for 96 h (L) S; (R) SA.

Fig. 8 – SEM photographs of top surface of sample after corrosion with fly ash and steam for 96 h (L) S; (R) SA.

40 mm; loading rate: 0.5 mm/min) in an Instron Universal Testing machine (Model 1123; Instron, Norwood, MA). Young's modulus was determined from the slope of the load–deflection curves using standard software (Instron Bluehill-2, Bucks, UK).

Results and discussion

The XRD analysis results of the fly ash as received and after calcination at 1000 °C for 96 h are presented in Fig. 1. No significant change in crystalline phases was noticed in the fly ash after calcination. The sample after corrosion tests exhibited neither surface cracks nor distortion of shape. The apparent changes in mass and porosity of the corroded samples are summarized in Table 1. The mass gain due to formation of cristobalite was compensated by the evolution of crystalline phases and formation of gaseous products as evident from XRD and SEM analyses. Maximum reduction of porosity was observed in the samples corroded in presence of steam due to enhanced oxidation of SiC. Aside from increasing the intensity of cristobalite other alkaline aluminosilicate was detected in XRD analysis of ash corroded samples as shown in Figs. 2 and 3. With increase of corrosion duration to 240 h further increase of cristobalite peak was noticed as presented in Figs. 4 and 5. But precise identification of crystalline phases was not possible due to the overlapping of many peaks of silicates with complex crystal structure.

The quantitative estimation of the amount of crystalline phases obtained by Rietveld analyses of XRD results are summarized in Table 2. The amount of cristobalite was increased from 19.6 to 25.2% for S sample after corrosion in presence

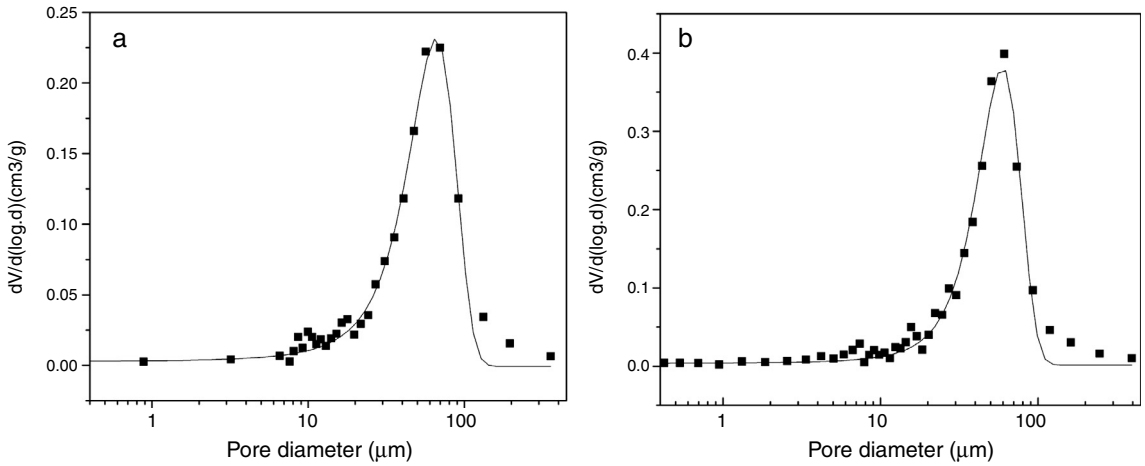

Fig. 9 – PSD pattern of S after corrosion with (a) fly ash and steam, (b) steam.

of steam, whereas in presence of fly ash amount of cristobalite was not increased instead additional ~12.9 wt% alkaline aluminosilicate was detected. Similarly the samples prepared with alumina additives showed increased amount of cristobalite after corrosion with steam. The results indicated that oxidation of SiC was reduced when samples was covered with fly ash.

The fly ash corroded samples were observed by SEM to investigate any morphological changes of these regions due to chemical interaction. It was observed in Fig. 6 that fly ash particles have entered into the pore. At higher magnification, aluminosilicate crystals were observed inside some pore. Some ash particles present in the interface with the sample surface particularly rich in glassy phase which can induce permanent sticking of these grains. Change in microstructure was more prominently visible in S sample. Many pores appeared at the grain boundaries mainly in the contacting bond phase region and also on the glassy surface of the grains. SEM microstructure of the samples calcined in presence of steam is presented in Fig. 7. Formations of cracks were clearly visible in both the steam corroded samples which may be due to the formation of increased amount of glass. It is reported that water vapour is more severe oxidizer than oxygen [10].

Fig. 8 shows the electron micrographs of steam and ash corroded samples. Cracks were generated in the contacting bond phase and crack propagation was arrested by the pores. The surface pitting was found on the glass layer indicated removal of volatile agents during corrosion at 1000 °C and volume shrinkage due to transformation of crystalline state. Formation of pores at the grain boundaries due decomposition of one or more components into gaseous products was also noticed by Monatznaro et al. [4] during corrosion of SiC based filter material with fly ash.

The pore size distribution pattern of the S filter material filter material after corrosion is shown in Fig. 9. The initial pore sizes was 71 μm but by corrosion at 1000 °C in fly ash and steam pore size of the filter material reduced to ~64 μm. The porosity of sample after corrosion with steam was found to be ~60 μm due to closure of porosity by formation of glass during corrosion.

The change of strength due to exposure of the filter material in presence of fly ash, steam and combination of steam and fly ash both are summarized in Table 3. The filter materials were found to remain stable during corrosion in presence of ash only and strength was found to increase after exposure for 96 h. The flexural strength was reduced to ~13 MPa and 23.6 MPa for S and SA samples respectively after 96 h of corrosion under steam. The strength reduction results are in good agreement with change in microstructure and XRD results. The rapid decrease of strength was found in samples after corrosion in presence of water vapour due to formation of excess glass phase, associated volume expansion and crack formation. The sample prepared with alumina showed better mechanical stability due to the presence of mullite in the bond phase. With further increase of corrosion duration to 240 h, flexural strength reduced gradually due to formation of higher amount of glass phase and depletion of crystalline phases. The residual strength of filter materials after 240 h of corrosion under steam and ash was found to be ~9.4 MPa and 16.6 MPa, respectively for S and SA samples. The microstructural changes decrease the strength of the filter material remarkably. In real operation conditions, thermal stress, mechanical stress combined with microstructural degradation may cause continuous degradation of strength and finally failure of the filter. To predict the safe life time of the filter more detailed studies are needed.

Table 3 – Effect of corrosion for 96 h on mechanical properties of filter materials.

Sample code	Room temperature mechanical strength							
	Initial strength of the filter material		After corrosion					
			In presence of fly ash		In presence of fly ash and steam		In presence of steam	
	Flexural strength (MPa)	Young's modulus (GPa)	Flexural strength (MPa)	Young's modulus (GPa)	Flexural strength (MPa)	Young's modulus (GPa)	Flexural strength (MPa)	Young's modulus (GPa)
S	28.0	29.7	31.6	30.2	15.33	17.04	13.3	18.4
SA	39.1	40.2	42.54	46.9	27.5	32.6	23.6	26.6

Conclusions

The corrosion behaviour of SiC ceramic filter materials in presence of steam, coal ash and both coal ash and steam was investigated at 1000 °C for 96–240 h. XRD analysis showed additional phase of calcium aluminosilicate after exposure in ash which appeared from the penetrated fly ash particles into the filter material. SEM studies also indicated that fly ash particles have entered into the pore and the binder was affected by heat treatment in presence of ash and steam. Ash particles were seen to be present in the interface with the sample surface particularly rich in glassy phase which induced permanent sticking of these grains. Many pores appeared at the grain boundaries mainly in the contacting bond phase region and also on the glassy surface of the grains. In presence of steam oxidation degree of SiC was increased and resulted higher amount of cristobalite. Significant reduction of flexural strength was obtained due to corrosion in steam due to formation of cracks at the bonding necks between SiC particles; however, the crack propagation was arrested by the pores which opposed further damage. But corrosion was less for samples covered with fly ash. On the basis of the present studies, it turns out that samples prepared with alumina additives showed better corrosion resistance. The preliminary test result support the ability of the ceramic filter material to be used as hot gas filter material, however their durability in aggressive atmosphere must also be studied to predict the durability of the material.

Acknowledgements

The authors would like to thank SERB, Department of Science and Technology, Government of India (GAP-0261) for financial support.

REFERENCES

[1] J.H. Choi, S.M. Keum, J.D. Chung, Operation of ceramic candle filter at high temperature for PFBC application, Korean J. Chem. Eng. 16 (1996) 823–828.
[2] T. Lücke, H. Fissan, The prediction of filtration performance of high efficiency gas filter elements, Chem. Eng. Sci. 51 (1999) 1199–1208.
[3] P. Pastila, V. Helanti, A.P. Nikkila, T. Mantyla, Environmental effects on microstructure and strength of SiC-based hot gas filters, J. Eur. Ceram. Soc. 21 (2001) 1261–1268.
[4] L. Montanaro, A. Negro, O. Frantz, P. Billard, R. Rezakhanlou, Corrosion of ceramic filters for hot Cleaning in thermal power plants, edited by Jessen T, Ustundag E 21 (2008) 561, http://dx.doi.org/10.1002/9780470294635.ch66.
[5] J.F. Zeivers, P. Eggerstedt, E.C. Zeivers, Porous ceramics for gas filtration, Am. Ceram. Soc. Bull. 70 (1991) 108–111.
[6] M.A. Alvin, Impact of char and ash fines on porous ceramic filter life, Fuel Process. Technol. 56 (1998) 143–168.
[7] M.A. Alvin, Characterization of ash and char formation in advanced high temperature particulate filtration systems, Fuel Process Technol. 44 (1995) 237–283.
[8] P. Pastila, V. Helanti, A.P. Nikkila, T. Mantyla, Microstructural determination in some SiC based hot gas filter materials, Adv. Appl. Ceram. 104 (2005) 65–72.
[9] P. Pastila, V. Helanti, A.P. Nikkila, T. Mantyla, Enviromental effects on microstructure and strength of SiC-based hot gas filters, J. Eur. Ceram. Soc. 21 (2000) 1261–1268.
[10] J.O. Elizabeth, Variation of the oxidation rate of silicon carbide with water–vapor pressure, J. Am. Ceram. Soc. 82 (1999) 625–636.